Deviations from the extended London model at high magnetic fields in $YBa_2Cu_3O_7$

E. Campillo [1,*] M. Bartkowiak [2] R. Riyat,[3] E. Jellyman,[3] A. S. Cameron,[4] A. T. Holmes [5] O. Prokhnenko [2] W.-D. Stein,[2] A. Erb,[6] E. M. Forgan,[3] and E. Blackburn [1]

[1]*Division of Synchrotron Radiation Research, Lund University, SE-22100 Lund, Sweden*
[2]*Helmholtz-Zentrum Berlin für Materialien und Energie, Hahn-Meitner-Platz 1, D-14109 Berlin, Germany*
[3]*School of Physics and Astronomy, University of Birmingham, Birmingham B15 2TT, United Kingdom*
[4]*Institut für Festkörperphysik und Materialphysik, Technische Universität Dresden, D-01069 Dresden, Germany*
[5]*European Spallation Source ERIC, P.O. Box 176, SE-221 00 Lund, Sweden*
[6]*Walther Meissner Institut, BAdW, D-85748 Garching, Germany*

(Received 3 March 2022; accepted 21 April 2022; published 11 May 2022)

We report on the evolution with the magnetic field and the temperature of the vortex lattice (VL) in fully oxygenated $YBa_2Cu_3O_7$ as studied by time-of-flight small-angle neutron scattering. Using the High Field Magnet/Extreme Environment Diractometer beamline at Helmholtz-Zentrum Berlin, we have obtained data up to 25.9 T—much higher than data available previously. Our VL structure results are consistent with the progressive suppression by the field of the superconductivity along the crystallographic **b** (CuO chain) direction and an accompanying shift of the nodal directions as the field is increased. The intensity of the diffracted signal reveals the spatial variation of magnetization caused by the VL (the "form factor"). Instead of a rapid falloff with the field, as seen in superconductors with smaller upper critical fields, we find that the form factor is almost constant with the field above ∼12 T. We speculate that this is due to Pauli paramagnetic effects.

DOI: 10.1103/PhysRevB.105.184508

I. INTRODUCTION

The vortex lattice (VL) in $YBa_2Cu_3O_{7-\delta}$ (YBCO) has been studied by small-angle neutron scattering (SANS) for more than 30 years, with the first observation made in a magnetic field of just 0.2 T [1]. Enormous advances in sample quality and SANS sample environments have allowed VL studies in YBCO to flourish and yield much information about superconductivity in this material [2–13]. In this paper, we present data on fully oxygenated YBCO in fields up to 25.9 T—experimental results obtained from the High Field Magnet/Extreme Environment Diffactometer neutron beamline at the Helmholtz-Zentrum Berlin [14–16]. SANS measurements of the VL structure as a function of the field and the temperature give us information on the penetration depth, the coherence length, and the superconducting gap structure of a given superconductor. In YBCO, SANS can also reveal the effective mass anisotropy, the VL melting, the VL pinning [13], and the field-induced nonlocality [12].

YBCO has an orthorhombic crystal structure, with CuO chains running along the **b** direction as well as the nearly square CuO_2 *ab* planes which are common to all cuprate superconductors. Upon cooling from the disordered high-temperature tetragonal phase, YBCO naturally becomes twinned with {110} twin boundaries separating domains with interchanged **a** and **b** axes. These twin planes act as strong pinning centers and control the VL orientation or structure observed in early SANS studies on twinned single crystals of YBCO [1–6,8–10]. Rotation of the twin boundaries out of the field direction has been somewhat effective in suppressing the pinning effects on the VL [2,8]. However, a more effective way to reduce the effects of the twin boundaries is to make measurements on a detwinned sample. In the first study to do so [7], the VL diffraction pattern showed a twofold symmetry, which reflected the *a-b* anisotropy of superconductivity in YBCO. The sign of this anisotropy showed that carriers in the CuO chains contributed to the superfluid density along the **b** direction.

The availability of high-quality detwinned single crystals of YBCO and high magnetic fields on SANS beamlines has allowed further study of this intrinsic VL structure, which shows that the field-induced VL structural transitions are *first-order*, unlike the *second-order* structural transitions observed in the twinned samples [8,10]. Here we extend the field range up to 25.9 T, obtaining more information on the intrinsic VL structure and superconducting state at high fields, including the temperature dependence at 25.9 T.

II. EXPERIMENTAL DETAILS

The fully oxygenated sample was a mosaic of aligned single crystals with total mass of ∼70 mg and an (overdoped) T_c of ∼89 K. It is further described in the Appendix. It was mounted with the crystal **c** axis parallel to the horizontal applied field and the **a** axis horizontal. The in-plane orientation of the mosaic was rotated by 90° with respect to that in

*emma.campillo@sljus.lu.se

previous work performed on the same sample at lower fields [12,13].

Our neutron measurements were carried out in two different experiments at the High Magnetic Field Facility for Neutron Scattering [14] which consisted of the High Field Magnet (HFM) [15] and the Extreme Environment Diffractometer (EXED) [16] at Helmholtz-Zentrum Berlin. The HFM was a hybrid solenoid magnet system with a maximum field of 25.9 T, making it the highest continuous magnetic field available in the world for neutron scattering experiments at the time. The direction of the horizontal magnetic field, and therefore of the sample, could be rotated relative to the incoming beam by up to 12°, limited by the size of the conical solenoid openings. The multipurpose HFM/EXED instrument operated in time-of-flight (TOF) mode, with a wide range of incident neutron wavelengths, maximizing the volume of reciprocal space that can be observed for a given orientation of the HFM. In our experiments, we chose this range to be 2.55–8.15 Å for the first experiment and 2.3–9 Å for the second one. Our data resulted from the use of this facility in SANS mode, enabling neutron measurements of mesoscopic magnetic structures in high fields.

The VL was prepared for observation at the base temperature of 3 K, by cooling the sample through T_c in an applied magnetic field. The VL quality is usually improved by oscillating the field value while cooling [13]. In the present case, the small variations of ∼30 mT from the magnet power supply served this purpose. For a given value of the applied field, and a given rotation of the HFM away from the incident beam direction, only one particular wavelength of neutron would be incident at the Bragg angle for diffraction by the VL. Neutrons of different wavelengths in the range supplied in TOF mode would be incident at angles away from the Bragg condition. Hence, the data at a single sample angle can contain a substantial part of the "rocking curve" of intensity of the VL Bragg spot. This contrasts with experiments using a monochromatic neutron beam, where the integrated intensity under the rocking curve is obtained by taking measurements at many different sample angles, rocking through the Bragg condition. In this work, TOF measurements were taken at just a few sample angles to check for consistency and to ensure that the entire rocking curve was covered by the wavelength spread [17]. The VL diffraction pattern shown in Fig. 1 was obtained by measuring at 3 K for both positive and negative magnet rotation angles, to give a complete first-order diffraction pattern from the VL. Background measurements were taken at the same angles above T_c and were subtracted from the measurements below T_c so that only the VL signal remained.

Data visualization and analysis were performed using the MANTID software package [18]. This allowed us to determine both the VL structure and the magnitude of the spatial variation of induction within the VL as a function of the applied magnetic field.

III. RESULTS

The VL structure can be described by the angle between two diffraction spots, ν, which is bisected by the **b*** direction. Figure 1 shows a typical diffraction pattern at 23 T and 3 K.

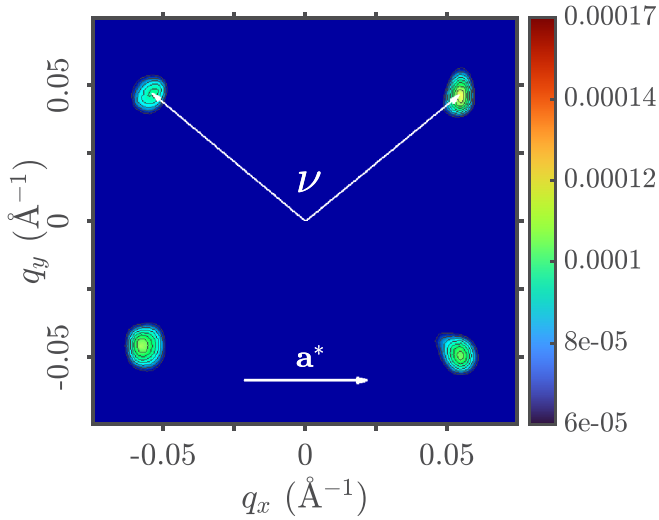

FIG. 1. A vortex lattice diffraction pattern at 23 T and 3 K. The opening angle ν is used to describe the structure of the vortex lattice. The plotted signal is a measure of the counts per pixel summed along q_z divided by the product of the incident beam intensity and the square of the neutron wavelength.

The incident beam has been masked out, and the data were smoothed using MANTID.

Figure 2(a) shows the opening angle ν as a function of the magnetic field. The circular points represent measurements from this study, and for comparison we have included data for the opening angle from previous measurements [12,13]. We see that the structure evolves continuously through a square VL at approximately 11.5 T and ν increases up to approximately 100° at the maximum applied field of 25 T. All measurements were taken at 3 K. In Fig. 2(b) the temperature dependence of the opening angle ν is displayed. At 25 and 25.9 T there are no apparent changes as a function of temperature in the opening angle which remains around 100°. The value at 19 T lies close to 95°, as expected from Fig. 2(a).

The VL form factor is the magnitude of a Fourier component of the spatial variation of the magnetic field within the VL. The form factor $F(\mathbf{q})$ for a diffraction spot with the wave vector $\mathbf{q}$ is related to the integrated intensity of a diffraction spot, $I(\mathbf{q})$, by the formula of Christen *et al.* [19]:

$$|F(\mathbf{q})|^2 = \frac{\Phi_0^2}{2\pi V\left(\frac{\gamma}{4}\right)^2}\frac{qI(\mathbf{q})}{\phi\lambda_n^2}, \tag{1}$$

where Φ_0 $(= h/2e)$ is the magnetic flux quantum, V is the illuminated sample volume, γ (=1.91) is the neutron magnetic moment in nuclear magnetons, and ϕ is the incident neutron flux per unit area in the neutron wavelength range $\Delta\lambda_n$ centered on λ_n. $qI(\mathbf{q})$ is derived from integrals over q_z of the neutron counts, $I(q_x, q_y, q_z, \lambda_n)\Delta\lambda$, which arrive in pixels of $\mathbf{q}$-space centered on (q_x, q_y, q_z). After background subtraction, the total integrated intensity is obtained from the region of $\mathbf{q}$-space containing a single diffraction spot and from the entire spectrum of neutron wavelengths used, which give a range of q_z. The VL peak width in q_z may be obtained by fitting a Gaussian line shape to the intensity summed over (q_x, q_y) as a function of q_z.

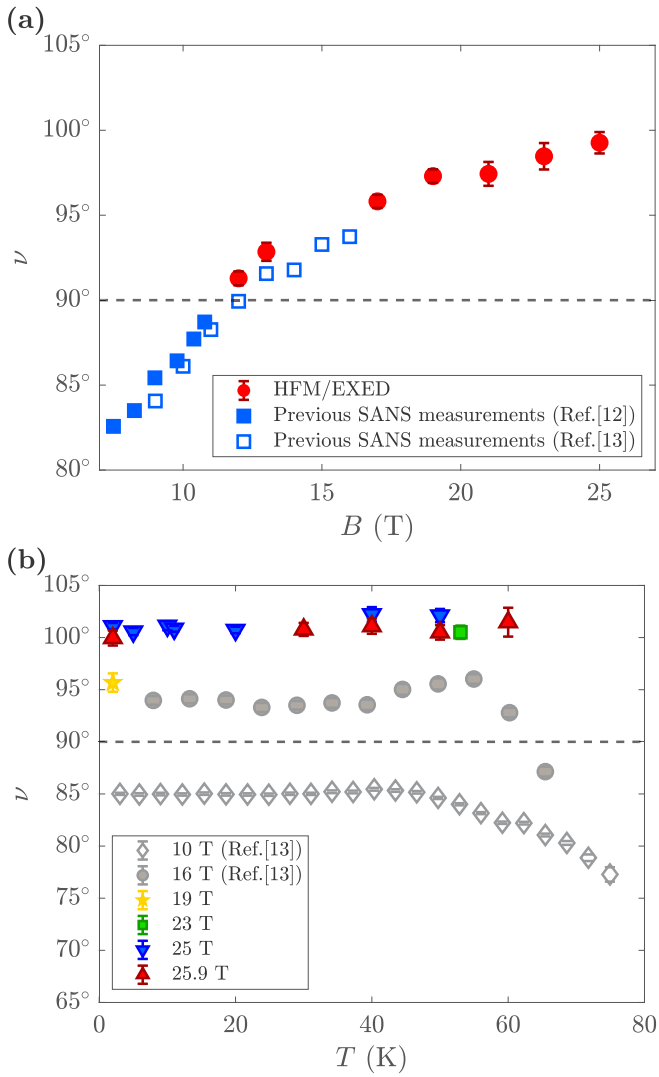

FIG. 2. (a) The evolution of the vortex lattice structure with the magnetic field at 3 K. The circular points are from this study while the filled square points are from a previous study [12] up to 11 T, and the open squares are included from Ref. [13]. (b) Variation of the opening angle with temperature at 25 and 25.9 T with two single points at 19 and 23 T. The diamond and circular points are from a previous study [13] and are provided for reference.

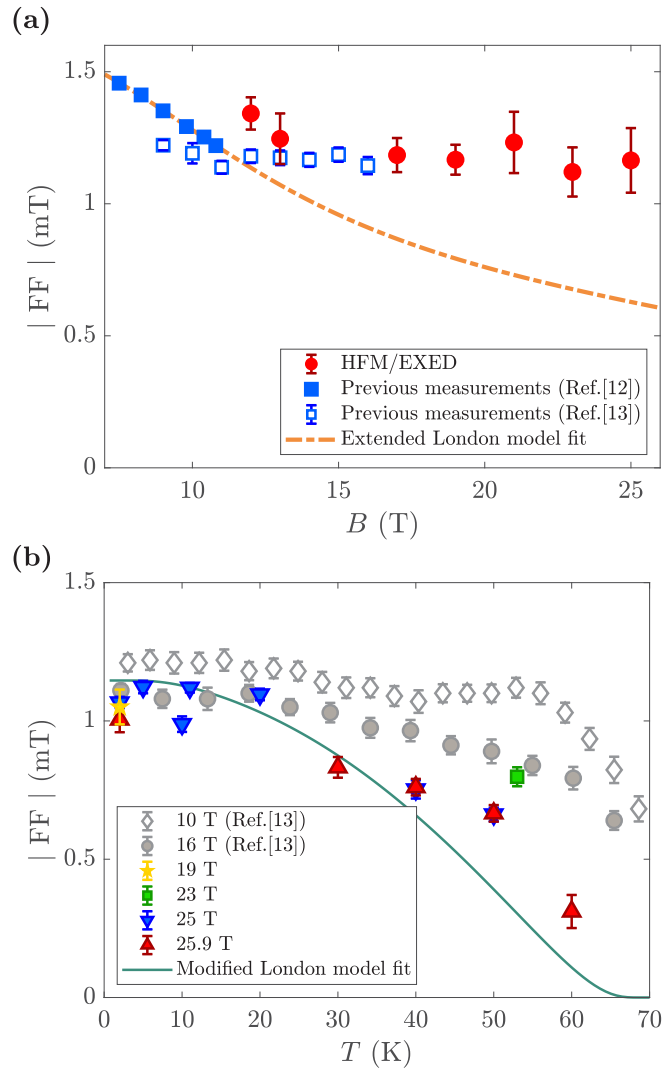

FIG. 3. (a) The vortex lattice form factor as a function of the magnetic field. The circular points are the new data reported here; the square points are drawn from Refs. [12,13]. The dashed line is a fit to the solid square points using an extended London model specified in the main text. (b) The temperature dependence of the vortex lattice form factor. The triangular and square points are from this work and the diamond and circular points from Ref. [13] are included for comparison. The solid line is discussed in the main text. Our data in this panel were taken in the second experiment, and the values of the form factor have been multiplied by a normalization constant of 1.5 to account for a loss in intensity observed due to a change in the detector between our first and second experiments. This normalization constant has been confirmed by a third experiment performed at the same facility with a 15% Ca-doped YBCO sample.

The dependence of the form factor on field and temperature is shown in Fig. 3. These results are discussed in more detail in the next section, along with the fits included in Fig. 3.

IV. DISCUSSION

To understand the evolution with the field of the VL structure at the base temperature, we must consider the whole field range that has been explored in fully oxygenated detwinned YBCO. First, at the lowest fields below ∼2 T, the VL structure is distorted hexagonal [8,11,12]. The distortion of ∼30% is essentially independent of the field, and its sign indicates an enhanced superfluid density along the **b** direction, which no doubt arises from the superconductivity of the carriers in the CuO chains, which run along this direction. The results in this field region may be completely described by anisotropic London theory [20], which applies when values of the London penetration depth λ_L and the vortex spacing are both much larger than the vortex core diameter $\sim\xi$, the coherence length. The stronger superconductivity along **b** is confirmed by zero-field measurements of the angles of the nodes in the order parameter [21]. In a purely d-wave superconductor, these would lie at exactly 45° to both **a** and **b** axes, whereas they are found to be closer to **a** (∼40°). As represented schematically in Fig. 4, this indicates enhanced superconductivity along **b**.

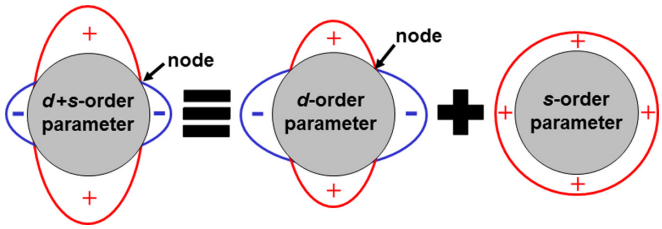

FIG. 4. Schematic representation of the variation of a $d + s$ superconducting order parameter around a cylindrical Fermi surface. In YBCO, such an admixture must arise because of the crystal structure and it has the same orthorhombic symmetry. It is seen that the nodal positions lie nearer the direction of weaker superconductivity. This will be the **a** direction at low fields and we propose that it is the **b** direction at high fields.

Between ∼2 and 6.5 T, the VL is also distorted hexagonal, but with the hexagon rotated by 90° relative to the low-field case [8,11,12]. The distortion falls with increasing the field, and this behavior has been discussed elsewhere [12]. For our present purposes, we merely emphasize the reduction of anisotropy with the field, which strongly suggests that the chain carrier superconductivity is suppressed by increasing the field to a much greater extent than that of the CuO_2 planes. We also note that within the London theory, the anisotropy of λ_L prescribes the distortion of the VL, but all *orientations* of the VL around the field direction are degenerate. Hence, the observed VL orientations in the low-field regions reflect rather weaker effects such as nonlocality [12], crystal defects, or the d-wave nodes.

Finally, above ∼6.5 T, the VL adopts a high-field centered-rectangular arrangement [8,11,12], continuously connected to what is observed in our field range. The nearest-neighbor vortex pattern is given directly by the pattern of diffraction spots around the main beam—rotated by 90° about the field axis. (This simple relationship represents the transformation between real and reciprocal lattices for the two-dimensional VL.) From Fig. 2(a), at approximately 11.5 T, the centered rectangle passes continuously through a square arrangement. At this specific field, the nearest-neighbor vortex directions are at 45° to the **a** and **b** axes. As the underlying crystal structure is orthorhombic, the square arrangement is not necessarily a special state, and as noted earlier, the nodes of the order parameter in zero field are at ∼40° to the crystal **a** axis, so YBCO is not a pure d-wave superconductor. Nevertheless, we would expect that calculations using the first-principles Eilenberger theory [23] applied to a d-wave superconductor are relevant. These predict a first-order transition from a low-field hexagonal VL to a high-field square VL, with the VL nearest-neighbor directions at high fields aligned with the nodes of the d-wave order parameter. It is reasonable to suppose that the first-order transition and the correlation between vortex and nodal directions still apply in our case.

Here, the opening angles change by less than ±5° from the square configuration (ν is between 80° and 100°) over the whole field range in which this high-field VL structure is observed. If we assume that in YBCO above ∼6.5 T the VL nearest-neighbor directions are closely linked to the nodal directions, then the variation of the VL structure with field shown in Fig. 2(a) may be interpreted as an indication of the movement of the nodal directions. First, at fields ∼7 T, we deduce that the nodes are closer to the **a** direction than to the **b** direction, which is consistent with the superconductivity being stronger along **b** than along **a**. This is clearly consistent in sign with the anisotropy in λ_L shown by the VL at low fields [12]. Furthermore, the value of ν at low fields tends towards that expected from direct measurement of nodal positions at zero field [21]. However as we have seen, the **b**-direction superconductivity is weakened by the field, and this trend is expected to continue above $B \sim 7$ T. This behavior is confirmed by the progressive movement of the VL structure towards square at ∼11.5 T. From the continuation of this trend at higher fields *past* the square configuration, we deduce that in this region superconductivity is stronger along **a**, giving nodal directions closer to **b**, as indicated in Fig. 4. This suggests that the superconductivity in the chain carriers is sufficiently weakened by the field that they tend to depair the plane carriers also.

We recognize that the decomposition of the carriers into chain and plane is a simplification, since they hybridize where the energy bands cross. Also, the electronic structure of the plane carriers is not quite the same along **a** and **b**, so there will be orthorhombic basal plane anisotropies, which may pull the VL nearest-neighbors slightly away from the nodal directions. Nonetheless, the variation of the VL structure with the field shows that the basal plane anisotropy is field dependent. It is far more likely that this is due to a field effect on the superconductivity, such as we have described, rather than on the underlying electronic band structure. We emphasize that at high fields, the VL diffraction pattern may be described as a distorted square with the stretching along the $\mathbf{a}^\star$ direction *increasing* with the field and reaching a maximum anisotropy at $\nu = 100°$ [see Fig. 2(a)]. On the other hand, for the two low-field VL structures, the diffraction pattern may be described as distorted hexagonal, with the stretching along the $\mathbf{a}^\star$ direction *decreasing* with the field. At low fields, the change of the VL structure with the field is clearly due to the field dependence of the anisotropy of the penetration depth. We would expect that in the high-field region, the VL distortion arises from a different mechanism, and our results strongly suggest that this is the change in the positions of the nodes in the order parameter. Nevertheless, the distortion of the VL at *both* low and high fields may be understood as a consequence of the *same* underlying phenomenon: the weakening of **b**-axis superconductivity with increasing the field. We cannot rule out other factors affecting variation of the VL shape with the field, but the nodal movement model gives a simple and comprehensive account of everything we observe.

We found surprising results upon observing the evolution with temperature of the vortex lattice structure at 25 and 25.9 T in Fig. 2(b). It has been predicted that the vortex lattice will return to the hexagonal arrangement upon approaching T_c. However, we observe that the VL angle ν is frozen at 100° and there is no evidence of a decrease, even at 60 K. During this experiment, the beam did not have enough intensity to measure the vortex lattice closer to its melting point. This may suggest that the change in the vortex lattice structure could happen even closer to T_c, which is in good agreement with what has been observed in previous SANS studies [12,13]. It

is important to point out that we did not observe any variation in the VL structure between 40 and 60 K, unlike previous observations at 16 T.

Now we turn to the field dependence and the temperature dependence of the form factor, shown in Figs. 3(a) and 3(b). For fields much less than B_{c2}, it is expected that the form factor will obey a London model, extended to include the effects of overlapping vortex cores of size $\sim\xi$, the coherence length. A key result of this work is that the observed continuous field dependence cannot be fitted by the extended London model. We find that the VL form factor remains more robust at high fields than would be expected from the suppression of spatial Fourier components of the field by VL core overlap.

To illustrate this, we have included in Fig. 3(a) a fit to an extended London model that represents our best attempt with this type of model. We find that the results of first-principles numerical calculations [23,24] of the form factor at $T << T_c$ are not in good agreement with the Ginzburg-Landau theory (which is only strictly valid close to T_c). Instead, they are closely approximated by an exponential factor [12]:

$$F(\mathbf{q}) = F_{\text{London}}(\mathbf{q})\exp(-cq^2\xi^2). \tag{2}$$

Here, c is a constant that is predicted to lie between 1/4 to 2. In agreement with previous practice [12,13], we chose c to be $\sim$0.44 (see the Appendix for a detailed justification for this choice). In Eq. (2), we have ignored any a-b anisotropy in ξ, because, throughout our field range, $\mathbf{q}$ remains approximately equidistant in angle from both axes. However, we have to take account of the anisotropy of the London penetration depth, because, by assumption, the degree of superconducting pairing, and hence one of the penetration depths in the basal plane, is field dependent. We therefore introduce values λ_a and λ_b, arising from supercurrents along the **a** and **b** directions, so that the London equation for the form factor becomes anisotropic:

$$F(q) = \frac{\langle B\rangle}{1+q^2\lambda^2} \rightarrow \frac{\langle B\rangle}{1+q_x^2\lambda_b^2+q_y^2\lambda_a^2}. \tag{3}$$

We have proposed that the value λ_b for the chain-direction currents is field dependent, as the chains become depaired. This happens over a field range around 10 T, so we take for this variation a purely phenomenological expression that has the expected qualitative behavior of flattening out at large and small fields,

$$\lambda_b^2(B) = \lambda_a^2\{1+0.4\tanh[(B-10\,\text{T})/(7\,\text{T})]\}. \tag{4}$$

Here, B is in Tesla, and we take the approximate width of the field range where λ_b is varying as 7 T. The factor 0.4 means that the two penetration depths differ by $\pm\sim$20% at low and high fields, with λ_b being shorter than λ_a at low field [12] and longer at high field.

To calculate the form factor as a function of field, we need the values of q_x, q_y, and q, which may be obtained from the positions of the diffraction spots. Alternatively, using only the value of B, the experimentally determined value of ν, and the fact that each vortex contains one flux quantum, one may write

$$q^2 = 4\pi^2 B/\Phi_0\sin(\nu);\ (q_x,q_y) = q[\sin(\nu/2),\cos(\nu/2)]. \tag{5}$$

The exponential in Eq. (2) for the form factor relies on the value of ξ, which may be related to the upper critical field using the Ginzburg-Landau relationship $B_{c2} = \Phi_0/2\pi\xi^2$. Hence, the experimental value of B_{c2} may be used to give the expected value for ξ. Alternatively, by substituting for ξ in Eq. (2), we may show that the cores give an approximately exponential falloff with the field:

$$\exp(-cq^2\xi^2) = \exp[-2\pi cB/B_{c2}\sin(\nu)]. \tag{6}$$

In Fig. 3(a), the dashed line represents the field dependence of F given by Eqs. (2), (3), and (4) from a fit to the data at 11 T and below, which gave $\lambda_a = 172.0(8)$ nm and $B_{c2} = 85(3)$ T. This fails to describe the high-field data, and in addition the value of B_{c2} is significantly lower than the reported value of around 120 T [25]. The falloff at high fields is much slower than that expected from the model and cannot be reproduced by the extended London model expressed in Eqs. (2), (3), and (4).

The VL perfection revealed by the present data (see the Appendix) is no better than that observed at low fields. Hence any effects of VL pinning in our field range should mimic a ξ with a value larger than that calculated from B_{c2}. However, Fig. 3(a) shows that the form factor is not falling off with the field as expected for any reasonable value of ξ and a constant value of λ_L. Furthermore, if we assume that the field is leading to the weakening of superconductivity along the CuO chain direction, which we represent using the field-dependent λ_b in Eq. (4), we can use a reasonable value of ξ (corresponding to $B_{c2} \sim 85$ T) to fit the data up to $\sim$11 T but not to higher fields.

Figure 3(b) shows the variation of the form factor with temperature at different fields. The values at high temperatures show a clear decrease with the field. We have fitted our temperature dependence assuming $d+s$ pairing [26], where

$$\Delta(T,\varphi) = \Delta_{0,d}(T)\cos(2\varphi) + \Delta_{0,s}(T), \tag{7}$$

where $\Delta_{0,s}(T) = -\cos(100^\circ)\Delta_{0,d}(T)$ to give nodes at the observed angle. We also assumed that $\Delta_{0,d}(0) = 2.14k_BT_c$ [26], with $B_{c2} = 120$ T [25] and $T_c = 70$ K at 25 T [27]. This model also fails to follow the temperature dependence of the form factor at high fields, especially at temperatures above 40 K, indicating again that the expected description breaks down. This suggests the influence of nonlocal effects [12] or larger values of Δ_0, but the limited quantity of data at high fields does not justify detailed analysis.

The intensity of the VL signal reflects the field contrast between the cores and their surroundings. We therefore conclude that, at high fields (although low relative to B_{c2}), there is a contribution to the spatial variation of the magnetic field in the VL in addition to that arising from supercurrents circulating around the vortices. This extra contribution must correspond to an additional magnetization of the vortex cores. This could arise as follows: The quasiparticles in the VL cores do not have to adopt the antiparallel spin arrangement of Cooper pairs, so the spins may align parallel to the magnetic field. This allows the formation of a Pauli paramagnetic moment in the core region [24]. Such effects must be present in all singlet-pairing superconductors, but will be negligible unless $\mu_B B_{c2} \geqslant k_B T_c$, so that the Zeeman energy of the electron spins is comparable with the zero-field energy gap. Pauli paramagnetic effects have been observed in heavy-fermion

materials such as $CeCoIn_5$ [28,29], $CeCu_2Si_2$ [30], a borocarbide [31], and an iron-based superconductor [32], but not to our knowledge in a high-T_c cuprate. Nevertheless, Pauli paramagnetic effects are expected in our sample, because it satisfies $\mu_B B_{c2} \simeq k_B T_c$.

V. CONCLUSIONS

Using neutron scattering at a unique instrument, we have observed diffraction by the lattice of magnetic flux vortices in a superconductor at higher fields than ever before. We have presented the evolution of the VL structure and form factor as a function of the field. We have considered the changes in these two aspects independently, as both properties appear to vary smoothly and changes in the VL structure do not usually lead to sharp changes in the form factor. There may be other explanations for the combined behavior observed, such as the onset of a new order parameter.

We have argued that the changes in the VL structure are those of a predominantly d-wave superconductor, with finer details determined primarily by the field dependence of the chain superconductivity. Specifically, we argue that the high magnetic fields preferentially disrupt the formation of Cooper pairs in the carriers traveling along the crystal's **b** direction (CuO chains) in this material. This is reflected by a change in the angular position of the order-parameter nodes in this orthorhombic $(d + s)$-wave material.

The intensity of the diffraction signal from the vortex lattice hardly falls off at high fields and the standard models for the form factor do not account for the observed field and temperature dependencies at these high fields. We take this as an indication of Pauli paramagnetic vortex cores.

Our results bode well for further studies at the high-field frontier when still greater steady fields become available at neutron scattering facilities.

ACKNOWLEDGMENTS

E.M.F. was supported by the Leverhulme Foundation. A.S.C. acknowledges support from the German Research Foundation (DFG) under Grant No. IN 209/3-1. We would like to thank Robert Wahle, Sebastian Gerischer, Stephan Kempfer, Peter Heller, Klaus Kiefer, and Peter Smeibidl for their support during the experiment.

APPENDIX

1. Sample

The sample, prepared at the Walther Meissner Institut, consisted of a mosaic of 11 coaligned single crystals of detwinned $YBa_2Cu_3O_7$ with a total mass of ∼73 mg. The crystals were grown from a molten flux of $BaCO_3$, CuO, and Y_2O_3 in $BaZrO_3$ crucibles [33]. They were detwinned through the application of uniaxial stress at a temperature of 500 °C for 24 h [34,35]. The crystals were then oxygenated close to the O_7 composition under an O_2 atmosphere of 100 bar at 300 °C for 150 h [36]. The filled CuO chains made the crystals slightly overdoped, but greatly reduced pinning by oxygen vacancies relative to that for an optimally doped sample. A crystal from the mosaic gave a zero-field T_c of 89.0 K by SQUID magnetometry in a field of 1 mT, with a 90% transition width of 2 K. Given the high purity of the samples, this spread in T_c suggests a slight spread in oxygen content across the mosaic. The mosaic was mounted on a 1-mm-thick aluminium plate, with the crystal's **c** axis perpendicular to the plate and the **a** direction coaligned between crystals.

2. Theoretical calculations of vortex lattice form factor

There are just two algebraic theories giving the expected form factor in the mixed state at fields not close to B_{c2}, but they are both of limited validity. One is the London theory, in which vortex cores are ignored, and hence this theory is only valid for very large $\kappa = \lambda/\xi$ (true for YBCO) and for

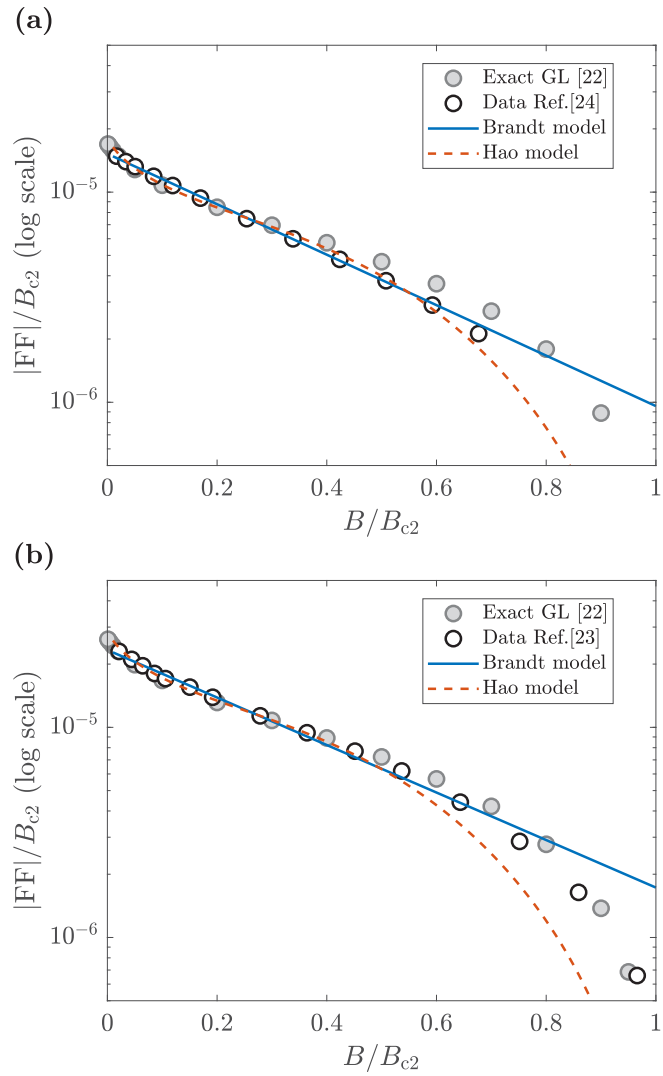

FIG. 5. Form factors versus field using several different theoretical approaches. Solid circles: The exact solution of the GL equations [22] (at a large value of $\kappa = 100$). Empty circles: The numerical solution of the Eilenberger equations. Dashed line: The Hao-Clem variational solution of the GL equations. Solid line: London model with exponential cutoff (the Brandt model). The form factors are calculated (a) for $T = 0.1\ T_c$ using results from Ref. [24] and (b) for $T = 0.5\ T_c$ using results from Ref. [23]. This is an updated version of the comparisons of GL solutions in Ref. [38].

$B << B_{c2}$. The other is the Ginzburg-Landau (GL) theory, developed as an expansion in powers of the order parameter near T_c and hence only numerically valid in this region. It does, however, give a *qualitative* picture of the mixed state at lower temperatures. To obtain an explicit expression for the predictions of the GL theory, Hao and Clem obtained a variational solution [37]. Later, Brandt established a numerical technique to obtain an *exact* solution of the GL equations for a VL at any fraction of B_{c2} [22]. However, there is a numerical *first-principles* method for obtaining the mixed state structure at both high and low temperatures, using the Eilenberger equations [23,24]. This can be used to test the validity of the GL equations away from T_c. In Fig. 5, we plot the results of all these methods versus the field for two different temperatures, together with a straight line given by Eq. (8) below. We see that at low temperatures [Fig. 5(a)] the Eilenberger result is very close to the straight line on a log-linear plot for fields $<0.5B_{c2}$. The Hao-Clem model deviates rather more from this line, particularly at high fields, while the exact GL solution oscillates about the line. In the higher-temperature case [Fig. 5(b)], both approaches deviate somewhat from the line, but again the Hao-Clem model deviates more strongly at high fields. A fitting of the low-field region, up to $0.5B_{c2}$, gives the following form:

$$F(\mathbf{q}) = F_{\text{London}}(\mathbf{q})\exp(-cq^2\xi^2). \tag{A1}$$

with $c = 0.44$. We get a better agreement with the model at $T = 0.1\ T_c$, but even leaving c as a free fitting parameter in the $T = 0.5\ T_c$ case we get a similar slope with $c = 0.41(2)$. This modified London model with exponential cutoff (or Brandt model) was also found to give a better fit to experimental data taken near the base temperature than the Hao-Clem expression. Further details may be found in Ref. [39].

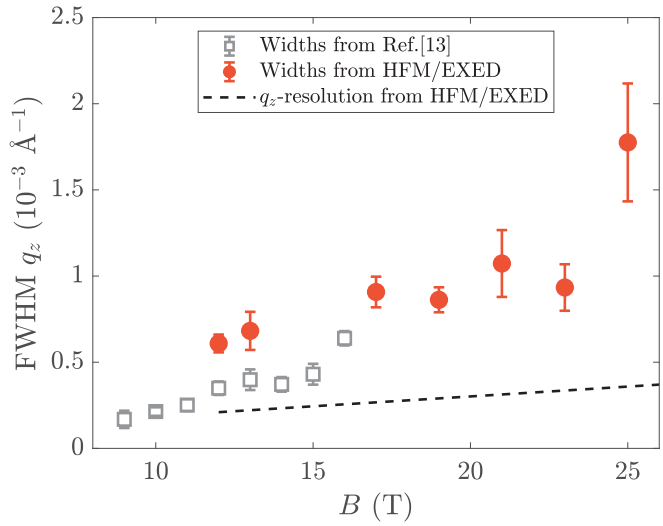

FIG. 6. The q_z width of the diffraction spots at the base temperature versus the field above 8 T. The empty square points are from a previous study [13]. The dashed line indicates the expected instrumental resolution for HFM/EXED.

3. Vortex lattice perfection

In addition to the quantities in the main text, we could also obtain the q_z widths of the diffraction spots, which are shown in Fig. 6. Above 17 T, the full width at half maximum (FWHM) is around $q_z \sim 10^{-3}$Å^{-1}, which is much larger than the instrument resolution. This q_z width corresponds to a correlation length along the vortex lines of $\sim 3 \times 10^{-7}$ m. Above 17 T, the q_z widths seem to increase with the field, following the trend given by data from previous studies [13]. The widths of the diffraction spots in the other two directions are largely instrument limited at a value of $\sim 8 \times 10^{-3}$ Å^{-1}, so they give little information about VL perfection.

[1] E. M. Forgan, D. M. Paul, H. A. Mook, P. A. Timmins, H. Keller, S. Sutton, and J. S. Abell, Nature (London) **343**, 735 (1990).

[2] M. Yethiraj, H. A. Mook, G. D. Wignall, R. Cubitt, E. M. Forgan, D. M. Paul, and T. Armstrong, Phys. Rev. Lett. **70**, 857 (1993).

[3] M. Yethiraj, H. A. Mook, G. D. Wignall, R. Cubitt, E. M. Forgan, S. L. Lee, D. M. Paul, and T. Armstrong, Phys. Rev. Lett. **71**, 3019 (1993).

[4] B. Keimer, W. Y. Shih, R. W. Erwin, J. W. Lynn, F. Dogan, and I. A. Aksay, Phys. Rev. Lett. **73**, 3459 (1994).

[5] B. Keimer, F. Doğan, I. A. Aksay, R. W. Erwin, J. W. Lynn, and M. Sarikaya, Science **262**, 83 (1993).

[6] E. M. Forgan and S. L. Lee, Phys. Rev. Lett. **75**, 1422 (1995).

[7] S. T. Johnson, E. M. Forgan, S. H. Lloyd, C. M. Aegerter, S. L. Lee, R. Cubitt, P. G. Kealey, C. Ager, S. Tajima, A. Rykov, and D. Mck. Paul, Phys. Rev. Lett. **82**, 2792 (1999).

[8] S. P. Brown, D. Charalambous, E. C. Jones, E. M. Forgan, P. G. Kealey, A. Erb, and J. Kohlbrecher, Phys. Rev. Lett. **92**, 067004 (2004).

[9] C. Simon, A. Pautrat, G. Poullain, C. Goupil, C. Leblond-Harnois, X. Chaud, and A. Brûlet, Phys. Rev. B **70**, 024502 (2004).

[10] J. S. White, S. P. Brown, E. M. Forgan, M. Laver, C. J. Bowell, R. J. Lycett, D. Charalambous, V. Hinkov, A. Erb, and J. Kohlbrecher, Phys. Rev. B **78**, 174513 (2008).

[11] J. S. White, V. Hinkov, R. W. Heslop, R. J. Lycett, E. M. Forgan, C. Bowell, S. Strässle, A. B. Abrahamsen, M. Laver, C. D. Dewhurst, J. Kohlbrecher, J. L. Gavilano, J. Mesot, B. Keimer, and A. Erb, Phys. Rev. Lett. **102**, 097001 (2009).

[12] J. S. White, R. W. Heslop, A. T. Holmes, E. M. Forgan, V. Hinkov, N. Egetenmeyer, J. L. Gavilano, M. Laver, C. D. Dewhurst, R. Cubitt, and A. Erb, Phys. Rev. B **84**, 104519 (2011).

[13] A. S. Cameron, J. S. White, A. T. Holmes, E. Blackburn, E. M. Forgan, R. Riyat, T. Loew, C. D. Dewhurst, and A. Erb, Phys. Rev. B **90**, 054502 (2014).
[14] O. Prokhnenko, P. Smeibidl, W.-D. Stein, M. Bartkowiak, and N. Stüsser, J. Large-Scale Res. Facil. **3**, A115 (2017).
[15] P. Smeibidl, M. Bird, H. Ehmler, I. Dixon, J. Heinrich, M. Hoffmann, S. Kempfer, S. Bole, J. Toth, O. Prokhnenko, and B. Lake, IEEE Trans. Appl. Supercond. **26**, 4301606 (2016).
[16] O. Prokhnenko, W.-D. Stein, H.-J. Bleif, M. Fromme, M. Bartkowiak, and T. Wilpert, Rev. Sci. Instrum. **86**, 033102 (2015).
[17] A. Pautrat, A. Brulet, C. Simon, and P. Mathieu, Phys. Rev. B **85**, 184504 (2012).
[18] O. Arnold *et al.*, Nucl. Instrum. Methods Phys. Res., Sect. A **764**, 156 (2014).
[19] D. K. Christen, F. Tasset, S. Spooner, and H. A. Mook, Phys. Rev. B **15**, 4506 (1977).
[20] V. G. Kogan, Phys. Rev. B **24**, 1572 (1981).
[21] J. R. Kirtley *et al.*, Nat. Phys. **2**, 190 (2006).
[22] E. H. Brandt, Phys. Rev. Lett. **78**, 2208 (1997).
[23] M. Ichioka, A. Hasegawa, and K. Machida, Phys. Rev. B **59**, 8902 (1999).
[24] M. Ichioka and K. Machida, Phys. Rev. B **76**, 064502 (2007).
[25] T. Sekitani, Y. H. Matsuda, and N. Miura, New J. Phys. **9**, 47 (2007).
[26] R. Prozorov and R. W. Gianetta, Supercond. Sci. Technol. **19**, R41 (2006).
[27] G. Grissonnanche, O. Cyr-Choinière, F. Laliberté, S. René de Cotret, A. Juneau-Fecteau, S. Dufour-Beauséjour, M.-E. Delage, D. LeBoeuf, J. Chang, B. Ramshaw *et al.*, Nat. Commun. **5**, 3280 (2014).
[28] A. D. Bianchi, M. Kenzelmann, L. DeBeer-Schmitt, J. S. White, E. M. Forgan, J. Mesot, M. Zolliker, J. Kohlbrecher, R. Movshovich, E. D. Bauer, J. L. Sarrao, Z. Fisk, C. Petrovic, and M. R. Eskildsen, Science **319**, 177 (2008).
[29] J. S. White, P. Das, M. R. Eskildsen, L. DeBeer-Schmitt, E. M. Forgan, A. D. Bianchi, M. Kenzelmann, M. Zolliker, S. Gerber, J. L. Gavilano, J. Mesot, R. Movshovich, E. D. Bauer, J. L. Sarrao, and C. Petrovic, New J. Phys. **12**, 023026 (2010).
[30] E. Campillo, R. Riyat, S. Pollard, P. Jefferies, A. T. Holmes, R. Cubitt, J. S. White, J. Gavilano, Z. Huesges, O. Stockert, E. M. Forgan, and E. Blackburn, Phys. Rev. B **104**, 184508 (2021).
[31] L. DeBeer-Schmitt, M. R. Eskildsen, M. Ichioka, K. Machida, N. Jenkins, C. D. Dewhurst, A. B. Abrahamsen, S. L. Bud'ko, and P. C. Canfield, Phys. Rev. Lett. **99**, 167001 (2007).
[32] S. J. Kuhn, H. Kawano-Furukawa, E. Jellyman, R. Riyat, E. M. Forgan, M. Ono, K. Kihou, C. H. Lee, F. Hardy, P. Adelmann, T. Wolf, C. Meingast, J. Gavilano, and M. R. Eskildsen, Phys. Rev. B **93**, 104527 (2016).
[33] A. Erb, E. Walker, and R. Flükiger, Phys. C (Amsterdam, Neth.) **258**, 9 (1996).
[34] C. T. Lin, W. Zhou, W. Y. Liang, E. Schönherr, and H. Bender, Phys. C (Amsterdam, Neth.) **195**, 291 (1992).
[35] V. Hinkov, P. Bourges, S. Pailhès, Y. Sidis, A. Ivanov, C. D. Frost, T. G. Perring, C. T. Lin, D. P. Chen, and B. Keimer, Nat. Phys. **3**, 780 (2007).
[36] A. Erb, A. A. Manuel, M. Dhalle, F. Marti, J. Y. Genoud, B. Revaz, A. Junod, D. Vasumathi, S. Ishibashi, A. Shukla, E. Walker, Ø. Fischer, R. Flükiger, R. Pozzi, M. Mali, and D. Brinkmann, Solid State Commun. **112**, 245 (1999).
[37] Z. Hao and J. R. Clem, Phys. Rev. B **43**, 7622 (1991).
[38] A. Yaouanc, P. Dalmas de Réotier, and E. H. Brandt, Phys. Rev. B **55**, 11107 (1997).
[39] C. J. Bowell, Ph.D. thesis, University of Birmingham, 2008.